N79-24009

DESIGN, DEVELOPMENT, AND FLIGHT OF A SPACECRAFT CHARGING SOUNDING ROCKET PAYLOAD

H. A. Cohen, C. Sherman and E. G. Mullen
Air Force Geophysics Laboratory

W. B. Huber
Tri-Con Associates, Inc.

T. D. Masek
Hughes Research Laboratories

R. B. Sluder
PhotoMetrics, Inc.

P. F. Mizera and E.R. Schnauss
The Aerospace Corp.

R. C.Adamo and J. E. Nanovich
SRI International

D. E. Delorey
Boston College

INTRODUCTION

The ejection of charged particles from a space vehicle creates a difference in potential between the vehicle and the ambient plasma. For steady state this potential difference causes a return current flow to the vehicle equal to the ejected current. Although there have been a number of flights during which energetic electrons have been ejected from rocket payloads, a relationship to predict the vehicle to ambient plasma potential difference created by an ejected electron current is still unknown. In fact, questions still remain as to which environmental parameters are critical in determining this potential difference. There is even far less experimental data available from payload flights in which positive, rather than negative charge has been ejected. A primary purpose for the flight of the Spacecraft Charging Sounding Rocket Payload was to create charging on the payload by the emission of both positive ions and electrons, and to determine the relationship between environmental parameters and changes in vehicle potential during periods of emission.

The design and choice of instrumentation for this Spacecraft Charging Sounding Rocket Payload were also influenced by the desire to test prototypes of some of the SCATHA satellite payloads: the positive and negative charge ejection system - the Transient Pulse Monitor (TPM) and the Rocket Surface Potential Monitor (RSPM). Data were desired on not only the operation of these instruments, but on their mutual interactions during operation. The flight of

the Spacecraft Charging Sounding Rocket payload also permitted a comparison of measurements made with SCATHA payloads to measurements made with other more standard techniques not available for SCATHA use.

INSTRUMENTATION

The launch vehicle for this payload was an Astrobee F rocket. The payload was divided into two electrically isolated sections by a non-conducting disk. The payload forward section, a cylinder 254 cm in length and 38 cm in diameter, contained all the vehicle diagnostic instrumentation. The rear section, a cylinder 41 cm in length and 38 cm in diameter, contained the payload recovery parachute, and was electrically connected to the front payload section only through a bipolar voltmeter. The instrumentation, classified into four broad categories, is listed and briefly described in Table 1.

A major operational problem that had to be overcome for this flight was the starting of the satellite positive ion beam system (SPIBS). The usual starting procedure for the system during testing in laboratory vacuum chambers was to pump down the source for at least 24 hours before trying to ignite the discharge. The actual initial ignition following this pump down has taken from five minutes to a half hour, depending on the previous exposure of ion system's hollow cathode and expellant assembly line to air. With the system continuously under vacuum conditions once the ignition has been initially started, reignition can be achieved in periods from ten seconds to one minute. This initial starting period requirement, acceptable for satellite flights, was completely unacceptable for a limited duration sounding rocket flight. The ignition problem was solved by pumping down the ion beam system on the ground before launch, and starting a discharge in the ion beam system 1/2 hour before launch. Close to launch the system was sealed off with the gas still flowing into the ion source and with the discharge still on. At the proper altitude, the cap was opened and the ion beam system allowed to emit high energy positive ions.

Ambient Electron Density

Launch date and time were set so that there could be a low number density, and a wide dynamic range of number densities of electrons over the expected altitude range for particle ejection, 120 to 250 km. These two compatible criteria were best expected to be fulfilled several hours after sunset during periods of quiet geomagnetic activity. Geomagnetic values and 3 hour predictions were obtained during the course of the launch day from the Air Force Global Weather Central (AFGWC). Environmental conditions at the time of the flight are summarized in Table 2.

An ionosonde located at the White Sands Missile Range was used to take vertical incident ionograms at 1 minute intervals during the flight period. The ionograms show that a sporadic E layer (E_s) with a peak n_e of approximately 10^4 electrons/cm^3 existed at an altitude near 104 km throughout the flight.

This E_s layer prevented a direct measurement of the ionosphere in the 104 to 220 km region. The n_e above 220 km was determined by an ionogram inversion technique developed by A. K. Paul and J. W. Wright (1963). The region between 102 and 220 km was modeled to correspond to the relative shape of a mid-latitude, magnetically quiet ($K_p = 0$) electron density profile determined from ionogram analysis by Wakai (1967). The model values were iterated until they agreed with the average valley n_e of 3.84×10^3 electrons/cm^3 determined from the ionogram analysis. This technique of determining n_e in the valley region does not give any small scale structure, but is generally accurate to approximately $\pm 20\%$. The n_e so determined is shown in Figure 3.

FLIGHT DESCRIPTION

The payload was launched from the White Sands Missile Range, New Mexico (lat 32°30'N, Long 106°30'W) on 21 January 1978 at 0900 UT (0200 LST). The flight trajectory is shown in Figure 1. The major flight events noted in Figure 1 are also listed in Table 3 in the sequence in which they occurred. Despin of the rocket produced a spin rate of approximately 1 rotation per 23 seconds for the data gathering interval (approximately 124 km on ascent to 111 km on descent). Separation of the payload from the rocket motor produced a tumbling of the payload through axial magnetic pitch angles ranging from approximately 5° to 180°.

With exceptions noted, all the instruments operated well; excellent data were obtained during the entire course of the flight with no telemetry losses. As planned, power to the payload charge ejection systems and sensing instrumentation was turned off at 111 km during descent. The payload parachute opened and operated successfully. During descent, into the lower atmosphere, the probe arm which was fully extended came off, and the gold plated surface material on the RSPM came off. On impact, the front disks of the ion beam source were broken. All the other equipment, specifically the camera and film, and the electronics of all the instrumentation were recovered in excellent reusable condition.

RESULTS

At launch plus 81 seconds when the RPA and TEP high voltage was turned on, high voltage arcing within the payload destroyed the electronic circuitry which controlled the RPA grid voltages. This caused the RPAs to function only as electrometers with the exception that RPA #1 had a +2 volt potential on the grid flush mounted with the payload skin. The arcing in the RPA, together with arcing produced later in the SPIBS, caused erratic behavior in the mode programmer throughout the flight, which in turn produced valuable unplanned, as well as the planned, SPIBS ejection modes. The arcing in SPIBS was first identified by characteristics on the output channels during laboratory tests. The times of arcing were corroborated during the flight by the Transient Pulse Monitor.

C-2

For a short time period after the SPIBS cap opening, a cathode to anode discharge was maintained in the ion source chamber. This permitted the ejection of 1.7 keV positive xenon ions at currents with values up to 370 μA. During the major portion of the flight, during ascent as well as descent, the cathode to anode discharge as the source of ions was replaced by the cathode to keeper discharge which resulted in ejected currents of 8 μA at .84 keV and 12 μA at 1.7 keV. A third unplanned SPIBS mode of 1 μA at 200 eV was also obtained. Electrons were emitted by the same ion beam system during the neutralizer filament bias mode. The ion beam system was operated from 125 km on ascent to 111 km on descent, a period of 350 seconds, and except for a short interval after the cap opening sequence, particles were emitted in a programmed cycle; the overall repetition rate was nominally six seconds, but some longer and shorter cycles were created due to SPIBS arcing. The electron beam system showed signs of cathode poisoning but did emit low currents of high energy electrons.

As shown in Figure 2, the sensors showed that the payload charged negatively and then positively with respect to the ambient plasma during the charge ejection of positive and negative particles respectively. As shown in Figure 3, the Thermal Emissive Probes, Bipolar-Intersegment Voltmeter, and Surface Potential Monitor responded to changes in vehicle potential in quite similar ways and had high negative correlations with ambient plasma density. All three sensor types gave repeatable results for ascent and descent. Figure 4 shows more clearly that although the sign and magnitude of potentials measured were the same, the actual values differed between the probes. These differences can be explained by the input impedance and time constants of the devices used to measure the voltages, the particle fluxes at the location of the probes, the magnitude of the voltages being measured, and the probe geometry. An analysis of these factors, using probe characteristics and load line diagrams, indicates in conformity with the majority of experimental results that at high voltages the Surface Potential Monitor should give the highest potential differences followed by the Bipolar Intersegment Voltmeter, and the Thermal Emissive Probes. The analysis shows that the probes should agree at lower voltages, and, in fact, at measured potentials less than 50 volts all three probe systems gave the same results.

The following is a summary of some of the results from the measurements of the probes during charged particle emission of the flight.

1. Unneutralized beams of positive and negatively charged particles can be emitted from a sounding rocket payload.

2. The payload can be charged either positively or negatively using charge ejection techniques.

3. There was excellent correlation between vehicle charging and ambient plasma density.

4. During periods of positive ion emission greater than 7 microamperes, vehicle charging levels were independent of vehicle pitch angle and ambient neutral particle density.

5. There was compatible and sometimes cooperative operation of the prototypes of instruments intended as SCATHA payloads.

REFERENCES

1. Paul, A. L., and Wright, J. W., J. Geophys. Res. 68, 5413-5420 (1963).

2. Wakai, N., J. Geophys. Res. 72, 4507-4517 (1967).

TABLE 1. - PAYLOAD INSTRUMENTATION

PURPOSE ....

Instrument

Method of Operation

I Charge Ejection

A. Electron Beam System

Electrons emitted from an indirectly heated oxide coated cathode maintained at negative potentials with respect to vehicle ground.

B. Satellite Positive Ion Beam System

Positively charged xenon ions extracted from a Penning discharge maintained at positive potentials with respect to vehicle ground. Electrons emitted from a heated filament kept at negative potentials with respect to vehicle ground.

II Measurement of the Payload Ground to Ambient Plasma Potential Difference

A. Thermal Emissive Probe

Coupled hot filament - passive probe mounted on an extendable boom. Outer shields of mounts driven to track probe voltages. A high impedance voltmeter measurement of probe to vehicle potential difference.

B. Bipolar Intersegment Voltmeter

A high impedance direct current equilibrium voltage measurement and a low impedance high frequency transient voltage measurement made between the isolated payload section and payload ground.

C. Surface Potential Monitor

Electrostatic measurement of the back surface potential of isolated kapton and gold surfaces. Also measurements of the current flow from the samples to vehicle ground.

D. Retarding Potential Analyzer

Measurement of the current to a collector placed behind a grid as a function of the retarding voltage applied to the grid.

III Vehicle Discharge Effects

A. Transient Pulse Monitor

TABLE 1. (Continued)

Radiation measurement of rate and amplitude of high frequency electric signals from discharges.

B. Camera-Arc Gap System

Photography of the dielectric surface gap between pairs of pointed conductors extended from the electrically isolated payload and the main payload sections.

C. Camera-Sheath Measurement System

Photography of a wedge of space adjacent to the payload skin.

IV Auxiliary Payload Measurements and Controls

A. Pitch Angle Measurement

B. Telemetry

C. Programmer

TABLE 2. - ENVIRONMENTAL FLIGHT CONDITIONS

Parameter	Condition
Magnetic Activity Index K_p	0 (Quiet)
10.7 cm Solar Flux	92
Wind	Light
Sky Visibility	Overcast
Solar Azimuth	71.3°
Solar Depression	64.9°
Lunar Azimuth	272.3°
Lunar Elevation	34.0°
Lunar Fraction Illuminated	92.2%

TABLE 3. - FLIGHT EVENTS SEQUENCE

TIME AFTER LAUNCH (Sec)	ALTITUDE (km)	EVENT
53	53	Motor Burnout
64	74	Despin
66	78	Motor Separation
69	83	Tip Blown
69	83	Boom Doors 1&2 Blown
69	83	Aerospace SSPM Door Blown
69	83	RPA #2 Door Blown
71	87	RPA #1 Door Blown
71	87	Camera Door Blown
81	105	TEP and RPA H.V. On
87	114	Electron Gun Cap Blown
94	125	Ion Gun Cap Blown
94	125	Camera On
95	127	500V TEP Boom Extended*
103	139	Ion Beam System On
157	205	Electron Beam System On
264	257.7	Apogee
443	111	Power Off

* 300V TEP Boom never fully extended. It may have remained totally inside the payload, or extended out to where the outer probe sphere was approximately 13 cm from the payload skin and the inner probe sphere was approximately 2.5 cm from the payload skin, or moved about somewhere between the limiting values.

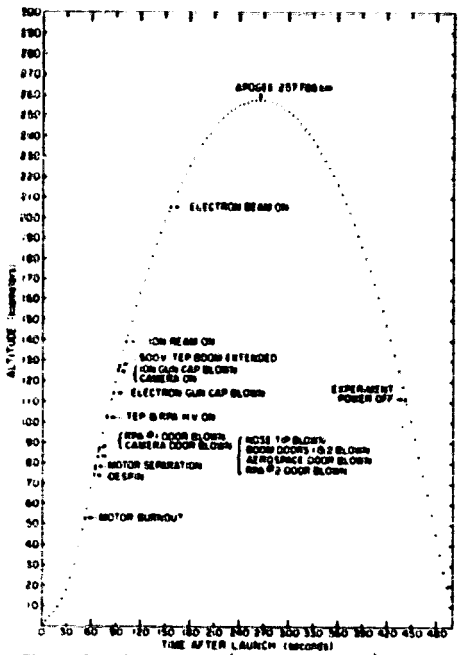

Figure 1. - Charging rocket A31.603 flight sequence.

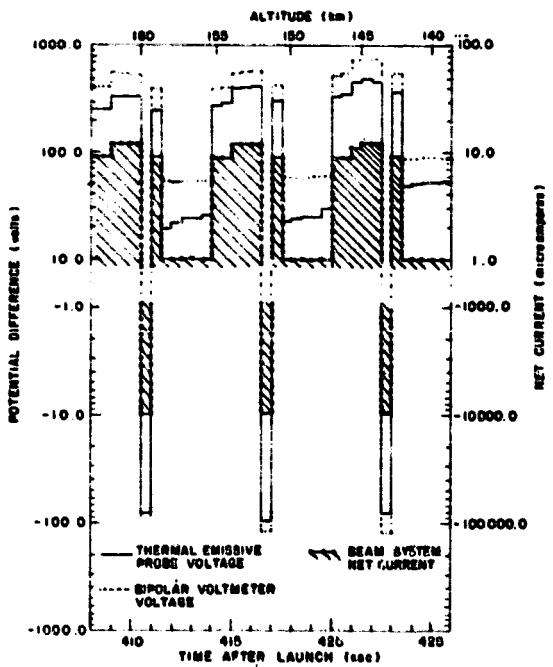

Figure 2. - Three program cycles.

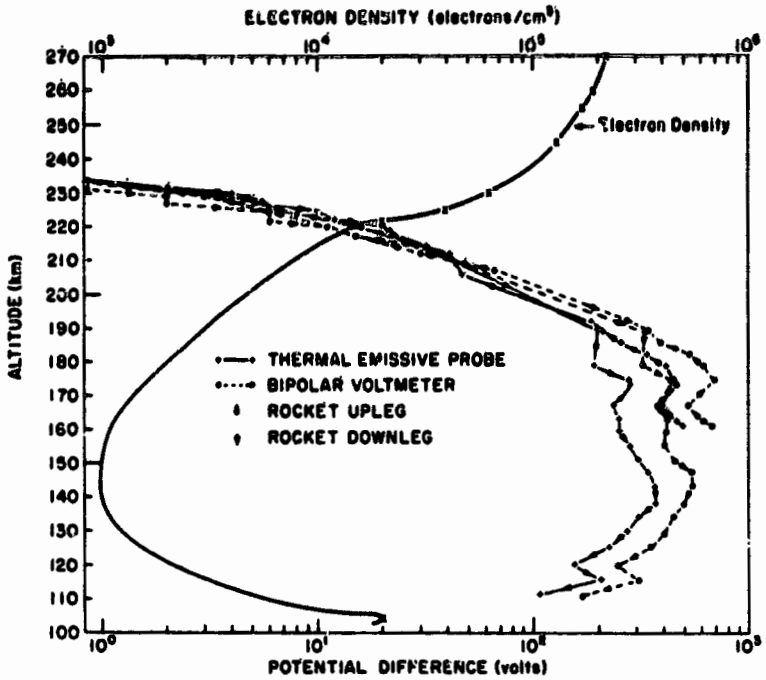

Figure 3. - Vehicle-to-ambient potential difference and electron density as function of altitude.

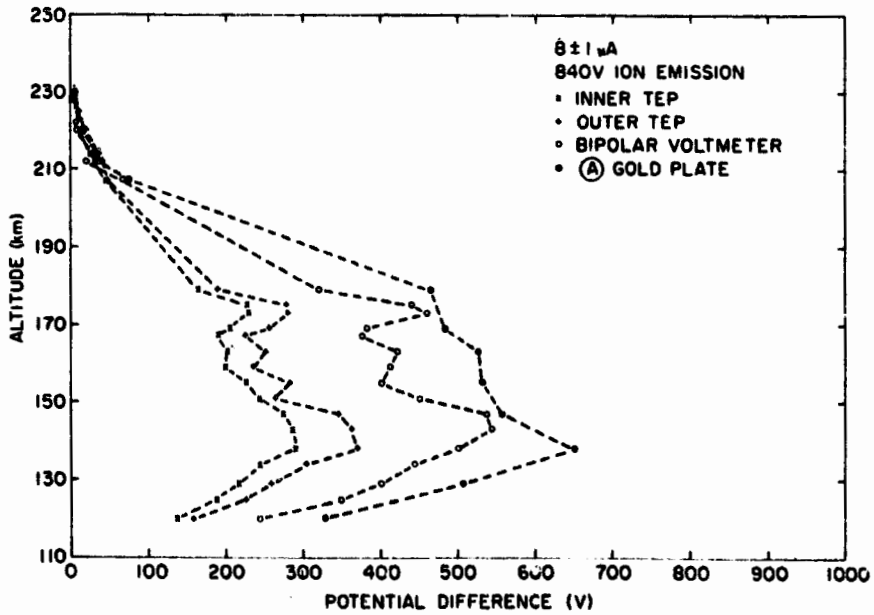

Figure 4. - Comparison of potential difference measurements.